

# Supporting Information: Spin dependent quantum transport interference in non-local graphene spin valves

M. H. D. Guimarães,<sup>\*</sup> P. J. Zomer, I. J. Vera-Marun, and B. J. van Wees

*Physics of Nanodevices, Zernike Institute for Advanced Materials, University of Groningen,  
The Netherlands*

E-mail: m.h.diniz.guimaraes@rug.nl

## Finite element calculations for the spin accumulation in the device

In order to calculate the classical spin accumulation expected for the device we used finite element simulations as implemented in the software COMSOL<sup>®</sup> MULTIPHYSICS. For this we solved the equations for spin diffusion:  $\nabla^2 \mu_s - \frac{\mu_s}{\lambda_s^2} = 0$  for our confined device geometry with a current of 100 nA applied between two electrodes with spin polarization  $P = 10\%$ . We assumed typical values for the square resistance of the graphene flake of  $R_{sq} = 1 \text{ k}\Omega$  which is in the same order of magnitude as in our experiment. Furthermore, we assumed a conservative value for the spin relaxation length of  $\lambda_s = 1 \text{ }\mu\text{m}$ . From the results of the simulation (shown in Fig. 1) we obtain a non-local spin valve signal of  $\approx 15 \text{ }\Omega$  which is in the same order of magnitude of the average experimental value for the non-local spin

---

<sup>\*</sup>To whom correspondence should be addressed

signal as a function of back-gate voltage presented in the main text ( $\Delta R_{nl}^{A-C} \approx 50 \Omega$ ). It is worth noting that this simulation uses a purely classical diffusion picture, which means that coherence effects are not included. Although such a picture describes well the spin transport of previous experimental studies on non-local graphene spin-valves<sup>1</sup> and also the average observed non-local spin signal, it fails to explain the oscillations in the non-local signal as a function of gate voltage.

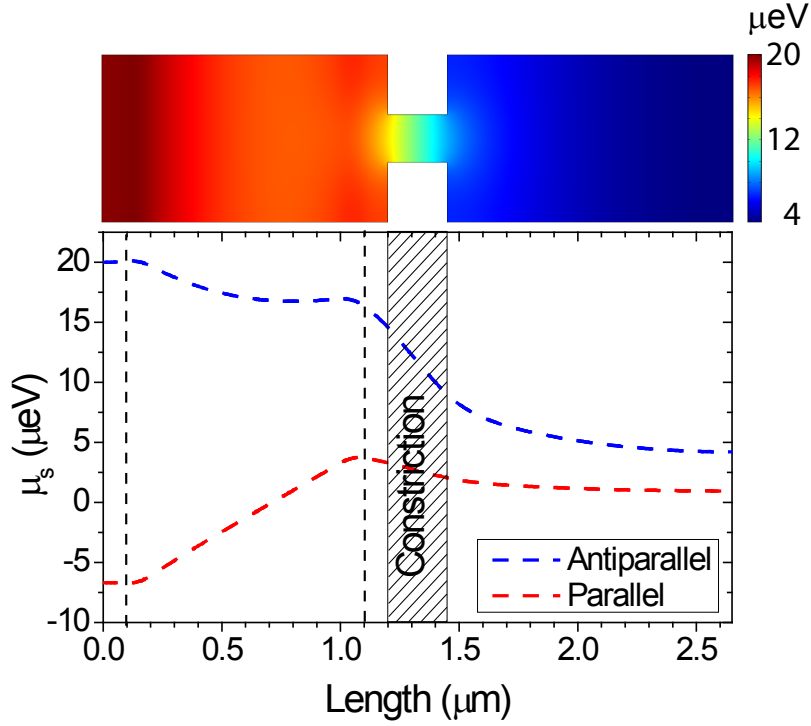


Figure 1: Finite element modelling of the classical spin accumulation in our device. On the top: device geometry with the location of the contacts shown by the dashed lines. The colour represents the spin accumulation according to the scale on the right for the case of anti-parallel alignment of the injection contacts. Bottom: Spin accumulation as a function of distance in the center of the device for both parallel and anti-parallel configuration of the injection electrodes.

# Effect of the stray magnetic fields from the side-gate electrode

In order to keep the contact interface as clean as possible we lowered the number of fabrication steps and fabricated the contacts and the side-gates at the same time. Therefore, the side-gate electrodes are also magnetic. To ensure that the stray magnetic fields arising from the side-gate electrode do not influence our results we performed finite element modelling of a cobalt bar of the same dimensions as the electrode in question. The bar is assumed to be uniformly magnetized up to its end, which gives a maximum estimate of the stray magnetic fields. In Fig. 2 we show the results of the simulation in the region of the center of the constriction ( $100 \text{ nm} \leq y \leq 300 \text{ nm}$ ).

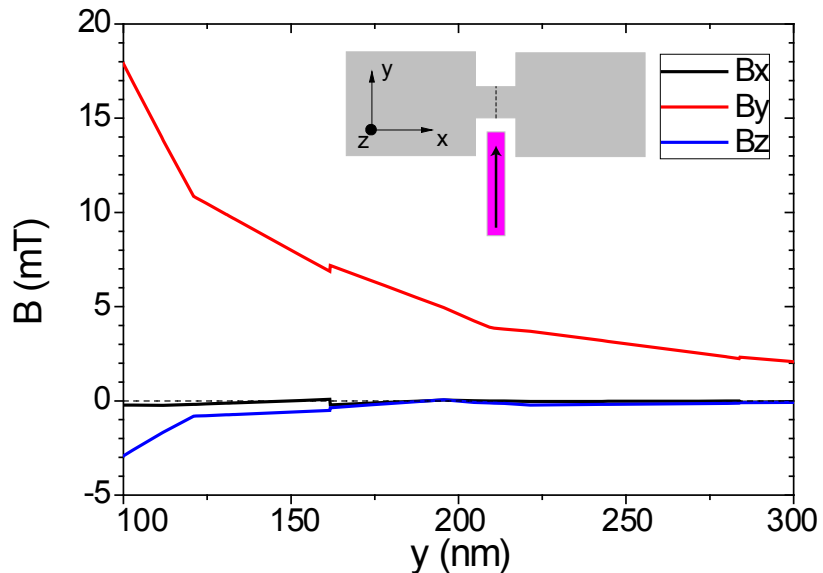


Figure 2: Components of the magnetic field in the x, y and z directions as a function of the distance for a cobalt bar of dimensions  $0.1 \times 10 \times 0.035 \mu\text{m}^3$ . The results are shown for a line across the center of the constriction as shown in the inset.

As can be seen, the values for the out-of-plane component ( $z$ ) is too small to create any orbital effect in the constriction. For the in-plane component, the maximum field is about 20 mT. This would create a Zeeman splitting of  $E_Z = 2.3 \mu\text{eV}$ , which is much smaller than the thermal energy  $E_T = 361 \mu\text{eV}$ . Therefore we do not expect that the stray fields from the

side-gate electrode would affect our findings.

To consider the effects of spin precession we have to take into account the out-of-plane component of the magnetic field  $B_z \leq 3$  mT which is too small to show any measurable effect in our measurements.

## Possibility of electric drift due to leakage current from the side-gate electrode

Here we consider the enhancement of the spin signal due to electric drift originating from a leakage current from the side-gate electrode. For a side-gate voltage  $V_{sg} = 2.5$  V the measured leakage current was below the limit of measurement of our electronic setup:  $I_{leak} < 0.01$  nA. Using this upper bound value for the DC current and the maximum square resistance of the device, we obtain an upper bound of the DC electric field of  $E < 0.1$  V/m. This value of electric field is 5 orders of magnitude lower than the values used to observe an effect of electrical drift on the non-local spin transport in graphene.<sup>2</sup> Therefore we do not expect an influence of electrical drift on our measured spin signals.

## Comparison to other devices

In total we measured 5 non-local spin-valves with different geometries (with or without a constriction and quantum dot), of which 3 were measured at low temperatures. From these 3 devices only the one with the constriction, which had the shortest channel length, showed Universal Conductance Fluctuations (UCF) of which the results are found in the main text. The two other devices, which had the shape of a quantum dot and longer channel lengths did not show UCF and also lacked a strong modulation of the non-local signal. Here we present the results for one of these devices.

The device consists of two large graphene pads connected via a quantum dot in the

center. The sample preparation was identical to the one described in the main text. The carrier density at the dot can be controlled using a local side-gate electrode similar to the one described in the main text. For measurements performed at 4.2 K we did not observe UCF nor a strong modulation of the spin signal for the whole range of gate voltages studied. In Fig. 3 we plot a typical measurement of the spin signal (grey), i.e. value of the non-local resistance in a parallel configuration of the electrodes minus the value of the anti-parallel configuration. For comparison we also show the local resistance of the device. As it can be seen, in the absence of UCF we do not observe neither a strong modulation nor a sign reversal of the spin signal.

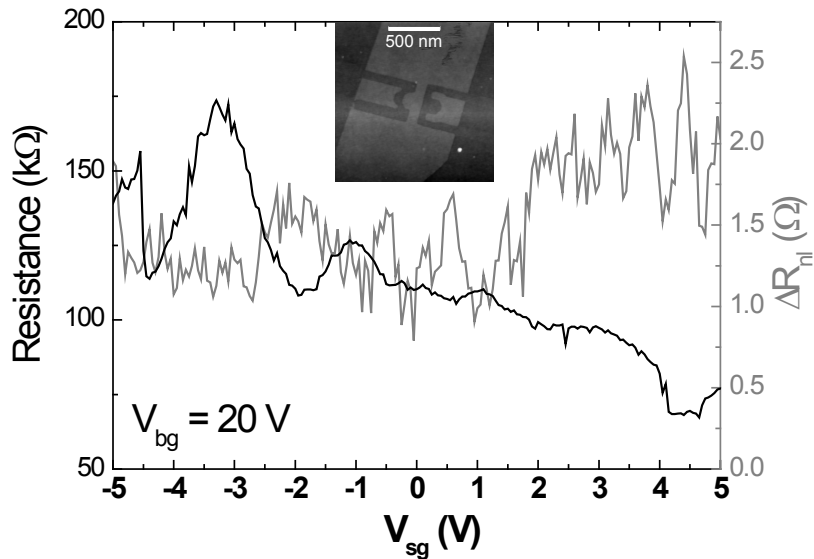


Figure 3: Four probe local resistance (black) and spin signal (grey) as a function of side-gate voltage for a back-gate voltage  $V_{bg}=20$  V. Inset: AFM image of the device before contact deposition.

## References

- (1) Vera-Marun, I. J.; Ranjan, V.; van Wees, B. J. *Nat. Phys.* **2012**, *8*, 313.
- (2) Józsa, C.; Popinciuc, M.; Tombros, N.; Jonkman, H. T.; van Wees, B. J. *Phys. Rev. Lett.* **2008**, *100*, 236603.